

# Corn Cob Xylan-based Nanoparticles: Ester Prodrug of 5-Aminosalicylic Acid for Possible Targeted Delivery of Drug

Samit Kumar and Yuvraj Singh Negi

Department of Polymer and Process Engineering,  
Indian Institute of Technology Roorkee,  
Saharanpur Campus, Saharanpur-247001 (U.P.) India;

## Abstract

Xylan, a green biopolymer extracted from agro-waste corn cob may be used as a tool to deliver drugs principally to the colon because of their timely retention in the physiological environment of stomach and small intestine and can only be degraded in colon by vast anaerobic microflora such as *Bifidobacterium*. Present research work relates to incorporate the drug molecule such as 5-aminosalicylic acid (5-ASA) into polymeric backbone of xylan by intermolecular covalent bond formation so that absorption of the drug is prevented in upper gastrointestinal tract (GIT) and minimizing the systemic side effects. The intermolecular covalent formation of 5-ASA to polymeric backbone of xylan was evaluated by means FT-IR, <sup>1</sup>H-NMR, solid <sup>13</sup>C-NMR spectroscopy. It may further be confirmed by TGA/DTA and powder X-ray diffraction. The resulting prodrug was self assembled into spherical nanoparticles with an average diameter of 54±11nm and 13±4nm as evaluated by means of AFM and TEM technique respectively. The prodrugs were synthesized which might be active against inflammatory bowel diseases, a novel idea towards advanced drug delivery by corn cob xylan will be discussed.

**Keywords:** <sup>1</sup>H-NMR, 5-ASA, AFM, FT-IR, Solid <sup>13</sup>C-NMR, TEM, Thermal analysis, Xylan biopolymer

## 1. INTRODUCTION

Corn cobs extracted from corn plant are either discarded as bio-waste or burnt as an application of low added value causing environmental concern, having an important constituents such as holocellulose, lignin and other bio-molecules in the approximate percentage of 73, 16 and 11 respectively [1]. Concerning specifically holocellulose, it has been demonstrated that such biopolymer presents a chemical composition of  $\alpha$ -,  $\beta$ -, and  $\gamma$ -cellulose in the proportion of 5.2:2.8:3.0 respectively on oven dry basis [1]. Xylan ( $\gamma$ -celluloses) is the most common hemicelluloses; represent more than 60% of the polysaccharides existing in the cell wall of corn cob [2], an alternative option for biomass utilization. Its main chain is constituted of D-xylopyranose units in the backbone linked through  $\beta$ -1, 4-glycosidic bonds whereas its side chain is constituted of 4-O-methyl-D-glucuronic acid (MeGlcA) and L-arabinose in the approximate ratio of 19:2:7 respectively [1-4].

Powder of extracted xylan have poor flowability because of irregular and rough structure [5], Hausner ratio, 1.68±0.01 [4], a ratio of less than 1.20 is an indicative of good flowability whereas a value of 1.5 or higher suggests a poor flow displayed by the material [6] and compressibility index, 40.77±0.0035% [4], is also called the Carr index, a value between 5 and 10, 12 and 16, 18 and 21, and 23 and 28 indicates excellent, good, fair, and poor flow properties of the material [4, 7]. In addition, it is generally believed that the flowability of powders decreases as the shapes of particles become more irregular [4, 8].

Xylan isolated from corn cobs is also known as corn fiber gum with a sticky behavior, used as an adhesive, thickener, and additive to plastics [9] that increases their stretch and breaking resistance as well as their susceptibility to biodegradation [10], as biofuel production [4, 11], as an

emulsifier and protein foam stabilizer during heating in the food industry [12], as an additives in papermaking [13] and textile printing [14], as a carrier for magnetite particles to protect from gastric dissolution when administrated orally [15], as a prodrug carrier for ibuprofen release in the pharmaceutical industry [16].

Regarding pharmaceutical applications, xylan has timely retention in the physiological environment of stomach and small intestine and can only be degraded in colon by vast anaerobic microflora stay alive in the range of 10<sup>11</sup>-10<sup>12</sup> colony forming units per milliliter (CFU/ml) [17] that fulfill its energy needs by fermenting various types of substrates that have been left undigested in the small intestine, e.g. di- and tri-saccharides, polysaccharide etc [18, 19]. For this fermentation, the microflora produces a number of enzymes such as  $\beta$ -glucuronidase,  $\beta$ -xylosidase,  $\alpha$ -arabinosidase,  $\beta$ -galactosidase, nitroreductase, azoreductase, deaminase and urea dehydroxylase [20]. Because of the presence of these biodegradable enzymes only in the colon, the use of bacterial degradable biopolymers for colon-specific drug delivery seems to be a more targeted approach as compared to others. It means these biopolymers shield the drug from the environments of the stomach and the small intestine and are able to deliver the drug to the colon [21]. On reaching the colon, they undergo assimilation by micro-organism or degradation by enzyme or breakdown of the polymer backbone leading to a subsequent reduction in their molecular weight and mechanical strength. Thus they are then unable to hold the drug entity any longer and thus release the drug in the colonic part of GIT [21].

Thus to protect the drug entity from upper GIT and avoid systemic side effects while administrated orally, various approaches have been developed to incorporate drug, including coating with biodegradable polymers, coating with

pH sensitive polymer, time dependent formulations, forming biodegradable matrices [22] and forming prodrug approaches [16, 23] is one more way to deliver drugs exclusively to colon because of biodegradable enzymes present only in the colon, where the drug molecules are covalently linked to the polymeric backbone. In prodrug approaches, polymeric or water-soluble carrier is employed to prevent absorption of prodrug in the upper GIT. Once delivered to the colon, the prodrug is presumed to be activated by the enzymes produced from the microflora [23, 24] should also modify the pharmacokinetics of the drug and obtain preferential localization, leading to a good sustained release system [25]. Thus, the objective of the present study is to synthesize and evaluate polymeric prodrug containing a non-steroidal anti-inflammatory drug, namely 5-ASA for sustained and site specific delivery.

## 2. MATERIALS AND METHODS

### 2.1. Raw material

Corn cob sample was collected from agricultural field locally (Dehradun, Uttarakhand, India) and it was milled into powder in a laboratory Wiley Mill, and fractions passing through 20 mesh (841 $\mu$ m) screens but retained on 80 mesh (177 $\mu$ m) screens was collected. Sample was air-dried, homogenized in a single lot to avoid compositional differences among aliquots, stored for compositional analysis and further treatment.

### 2.2. Extraction of Xylan

The xylan was extracted from corn cobs following the technique as reported elsewhere [2] with some modifications. After grinding, the dried corn cobs were dispersed in water under stirring for 24h. Then, sample was treated with acidified sodium chlorite (CH<sub>3</sub>COOH/NaClO<sub>2</sub>) in order to remove lignin and other impurities. The xylan was then extracted from the delignified pulpy mass by using 4% (w/v) sodium hydroxide solution. During extraction, the system was maintained under moderate stirring at 60°C for one hour. Afterward, the extract was neutralized with acetic acid and xylan was separated by settling down after methanol addition subsequently, several washing steps were performed by using methanol. Finally, the sample was filtered and dried at 60°C in vacuum oven. The characterization process was made from the same single bulk of polymer. Xylan extraction from corn cob yielded 10  $\pm$  1.6% (n=3) on oven dry basis which is slightly less than [4].

### 2.3. Synthesis of 5-N-formylaminosalicylic acid (5-fASA)

In the present experiment, 24.7g (0.161mol) of 5-ASA was dissolved into 247ml of 98% formic acid, refluxed for 30 minutes and then excess of cold distilled water was added for

precipitation. The precipitates were filtered, washed several times with cold distilled water and dried in vacuum oven at 60°C up to a constant weight (24.084g, 82% yields), mp: 267.7°C, analogous to Jung et al., 1998 and Zou et al., 2005 [22, 23], mp: 248-251.19°C. The reaction scheme may be illustrated as fig.1.

The percentage yield of 5-fASA was calculated as follows

$$\% \text{ yield} = (\text{Observed weight of 5-fASA} / \text{Theoretical weight of 5-fASA}) \times 100$$

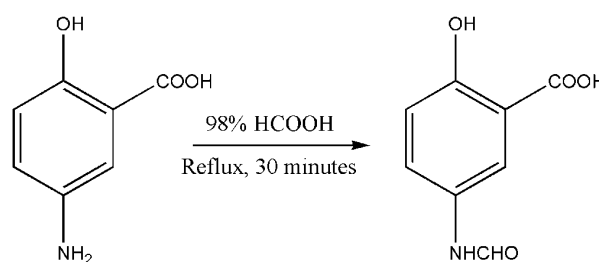


**Fig.1 Schematic representation of synthesis of 5-fASA (Zou et al., 2005)**

### 2.4. Synthesis of xylan-5-ASA ester conjugates

Xylan is constituted of D-xylopyranose units, linked through  $\beta$ -1, 4-glycosidic bonds. Thus, only two hydroxyl groups (at 2 and 3 positions) are free for modification and therefore only two types of molar ratio such as 1:1 and 1:2 of xylan and 5-fASA were taken for esterification in the present study as shown in table 1.

To the solution of 5-fASA (2g, 0.011mol) in DMF (55ml), CDI (1.95g, 0.012mol) was added slowly and reacted for 1 hour at room temperature, and then xylan (1.44g, 0.011mol) in DMSO (55 ml) was added drop wise. To the reaction mixture, triethylamine (1ml) was added and stirred for 24 hours at room temperature. To produce precipitates, 1N HCl or acetone was added in excess. The obtained precipitates were hydrolyzed with 0.1N HCl for 10 minutes at 80°C. The obtained product was washed several times with acetone to remove impurities, dried in vacuum oven at 60°C up to a constant weight. The synthesized ester conjugates (prodrugs) were obtained as 95% and 82% yields respectively as shown in table1. The percentage yield of xylan-5-ASA ester conjugates were calculated as follows

$$\% \text{ yield} = (\text{Observed weight of xylan-5-ASA} / \text{Theoretical weight of xylan-5-ASA}) \times 100$$

**Table 1: Shows the percentage yield and degree of substitution of xylan-5-ASA ester conjugates during two molar ratio**

Samples	Yield (%)	UV absorbance (338nm)	$x=(y+0.006)/0.020$ ( $\mu$ g/ml)	Drug content (mg)/g of Prodrug	Degree of substitution (DS)
Xylan-5-ASA_1:1	95.37	8.92	446.40	511.69	51.17
Xylan-5-ASA_1:2	82.51	8.74	437.05	665.32	66.53

### 2.5. Nanoparticles preparation

Synthesized prodrug was ground in Mixture Mill (Retsch, MM-400) to form free flowing powder. The powder was analyzed for particle size estimation by forming the suspension in water with sonication. One drop of this suspension was placed on glass slide for the analysis of particle size by SEM and AFM. One drop of the suspension was also placed on carbon coated copper grid for the analysis of particle size by TEM technique after evaporation of the solvent.

### 2.6. Estimation of drug content in xylan-5-ASA ester conjugates

To evaluate the authentic amount of drug such as 5-ASA in the polymeric backbone of xylan, it was necessary to carry out a fast hydrolysis of drug from xylan polymeric system. It was assumed that the xylan-5-ASA 1:1 ester conjugate (molecular Weight 267g) when hydrolyzed, gives 153g of 5-ASA. Therefore, 25mg of 5-ASA is released from 43.625mg of the same conjugate, was taken in 50ml of 1N NaOH solution so that the concentration of 5-ASA become 0.5mg/ml, left for 1h. Similarly, 32.925mg of xylan-5-ASA 1:2 esters conjugate was taken in 50ml of 1N NaOH solution and left for the same time. Simultaneously, 25mg of pure 5-ASA was also taken separately in 50ml of 1N NaOH solution for making standard curve. The different working standards namely from 0.025 $\mu$ g/ml to 100 $\mu$ g/ml were prepared by appropriate dilutions and assayed by an UV/VIS spectrophotometer at  $\lambda_{\max}$ 338nm for making standard curve.

The equation was obtained as

$$y=0.020x-0.006, R^2 = 0.999$$

Where, x is the concentration of 5-ASA and y is UV absorbance at  $\lambda_{\max}$  338nm.

### 2.7. Degree of substitution (DS)

Degree of substitution was defined as mg of 5-ASA bound in 100mg of xylan-5-ASA ester conjugate. It was determined by measuring the amount of sodium 5-aminosalicylate by UV absorbance at  $\lambda_{\max}$ 338nm, which was released when 100 mg of xylan-5-ASA ester conjugate was placed in 1N NaOH solution for 1h. Degree of substitution can easily be adjusted by varying the molar ratio of xylan and 5-fASA as shown in Table 1.

### 2.8. In vitro release studies of 5-ASA

The release of 5-ASA was followed as a function of time. In-vitro release of drug was evaluated with pH 7.4 and 1.2 in the phosphate buffered saline (PBS) and 0.1N HCl solutions at  $37\pm 1^\circ\text{C}$  with shaking at  $100\pm 5$  rpm and assayed by an UV/VIS spectrophotometer at  $\lambda_{\max}$ 338 and 300 nm respectively. Five-milliliter samples were taken from the dissolution medium at scheduled time intervals using a graduated pipette. At each sampling point 5ml of blank solution having same pH was added to the dissolution vessel. The concentration of 5-ASA at each sampling point was measured spectrophotometrically at 300 and 338 nm for 0.1 N HCl, pH 1.2 and PBS, pH 7.4 respectively.

### 2.9. Characterization

Fourier Transform-Infrared (FT-IR) spectroscopy was performed using a Nicolet spectrophotometer. Samples

were oven dried at  $105^\circ\text{C}$  for 4 h, mixed with KBr in a ratio of 1:200 mg (Xylan: KBr) and pressed under vacuum to form pellets. The spectrum was taken in the range of  $4000\text{-}500\text{ cm}^{-1}$ .

Proton-Nuclear Magnetic Resonance Spectroscopy ( $^1\text{H-NMR}$ ) was performed on a Bruker 500 Ultrashield spectrometer operating at 500MHz, with TFA-d as solvent and tetramethylsilane (TMS) as internal standard with 16 scans.

Solid  $^{13}\text{C-NMR}$  Spectroscopy was performed on a Bruker Biospin Switzerland, Avance III 700 Ultrashield spectrometer operating at 700 MHz with 1529 scan.

Powder x-ray diffraction (PXRD) of the sample was recorded on a Bruker AXS D8 Advance diffractometer with a scanning rate of  $1^\circ\text{C}/\text{min}$  with  $\text{CuK}\alpha$  radiation source ( $\lambda = 1.54060\text{\AA}$ ) operating at 40 kV and 30mA, in  $2\theta$  range from  $5^\circ$  to  $60^\circ$ . Finely powdered samples were placed in the central cavity of sample holder made up of PMMA (Poly Methyl Methacrylate).

TGA, DTG and DTA were carried out simultaneously by using EXSTAR TG/DTA 6300 thermogravimetric analyzer. The resolution of this instrument is  $0.02\mu\text{g}$  as a function of temperature. Runs were carried out at heating rates  $10^\circ\text{C min}^{-1}$  from ambient temperature to  $900^\circ\text{C}$  under high purity nitrogen at a flow rate of  $200\text{ ml min}^{-1}$ . Thermal analysis techniques such as thermogravimetry (TG), derivative thermogravimetry (DTG) and differential thermal analysis (DTA) are widely used to measure the thermal stability and pyrolysis behavior of polymers in different conditions.

Field Emission-Scanning Electron Microscopy (FE-SEM) analysis was performed, using a FEI Quanta 200F microscope. The samples were dispersed in water, mounted on glass slide, heat fixed and observed at 15 to 20 kV after gold coating.

Atomic Force Microscopy (AFM) was carried out with NT-MDT NTEGRA. The samples were dispersed in water, mounted on glass slide, heat fixed and observed with AFM without any further modification.

High-resolution Transmission Electron Microscopy (TEM) was carried out with FEI Technai G2 F20 microscope at 200 kV. For TEM observation, the samples were prepared in methanol at 100  $\mu\text{g}/\text{ml}$  concentration and dispersed in an ultra-sonicator for ten minutes. The samples for TEM analysis were obtained by placing a drop of the colloidal dispersion containing prodrug nanoparticles onto the carbon-coated copper grid. They were dried at room temperature and then examined using the TEM without any further modification

## 3. RESULTS AND DISCUSSION

The de-waxed 10g corn cob powder was delignified with acidified  $\text{NaClO}_2$  solution at  $70^\circ\text{C}$  without degrading cellulose and hemicellulose.

Reaction involved:



The  $\text{ClO}_2$  act as bleaching agent, removing coloring material and lignin however, delignification process could not dissolve the whole lignin. It is found that the cellulose microfibril in a hydrophobic matrix is physically shielded by lignin and lignin is covalently bonded with cellulose and hemicellulose. Therefore, lignin could not be separated completely from cellulose and hemicelluloses [26]. Delignified product was treated with 250ml of 1N NaOH solution and residual lignin was removed by alkali treatment that cleaves the  $\beta$ -alkyl-aryl ether bonds ( $\beta$ -O-4 linkages) in lignin via the formation of an epoxide intermediate with an intramolecular nucleophilic displacement of the  $\beta$ -phenoxide by either the  $\alpha$ - or  $\gamma$ -alkoxide formed from the alcohol in strong base [3]. Subsequent nucleophilic attack by hydroxide cleaves the epoxide ring and produces a tri-hydroxyl propane structure. Thus the residual lignin was removed by NaOH treatment and xylan was extracted from alkaline filtrate by precipitation with 1N acetic acid, settling down with methanol, several washing steps were performed by using methanol. Finally, the sample was filtered and dried at  $60^\circ\text{C}$  in vacuum oven. The characterization process was done from the same single bulk of polymer.

### 3.1. FT-IR Spectroscopy of corn cob extracted holocellulose and xylan

FT-IR spectroscopy is an effective tool for studying the physico-chemical and conformational properties of the polysaccharides. The main absorption band of FT-IR spectra of the extracted holocellulose and xylan are shown in fig.2. The analysis of FT-IR data shows that the holocellulose has most significant absorption band at  $1734\text{cm}^{-1}$  attribute to C-O stretching of carbonyl group [27] which was disappeared in xylan may be due to the removal of side chain of acetyl group of acetylated xylan by alkali treatment at elevated temperature ( $70^\circ\text{C}$ ). The absence of absorption band between  $1450\text{cm}^{-1}$  to  $1600\text{cm}^{-1}$  may further confirm the complete removal of lignin during extraction process and thus, based on the above observations the isolated hemicellulose was a homoxylan.

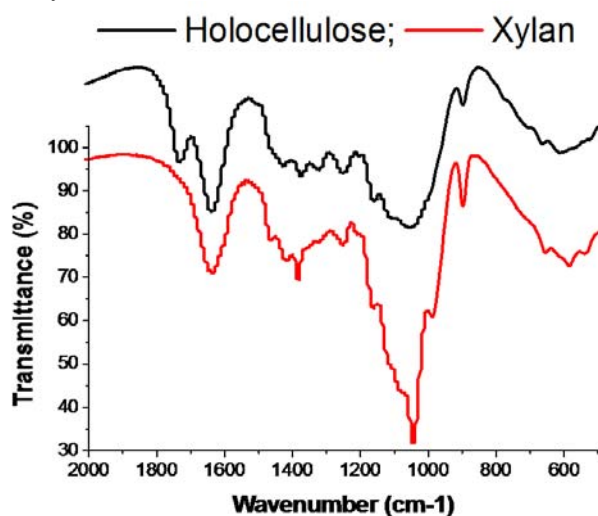


Fig.2 Shows the FT-IR spectrum of holocellulose and xylan

A sharp band at  $1633\text{-}1642\text{cm}^{-1}$  was attributed to H-O-H stretching, which occurs mainly in the amorphous state, and crystalline spectra measured in KBr which belongs to the absorbed water molecules [4, 28]. The band at  $1430\text{cm}^{-1}$  assigned to H-CH and -OCH in-plane bending vibrations in both holocellulose and xylan component [29]. In addition, an absorption band near  $1383\text{cm}^{-1}$  is detected owing to the C-H bending vibration present in hemicelluloses whereas, band near  $1375\text{cm}^{-1}$  is attributed due to C-H bending vibration present in holocellulose [29]. The presence of the arabinosyl side chains is characterized by a low intensity shoulder at  $1167\text{cm}^{-1}$  corresponding to the C-O-C vibrations in the anomeric region of hemicelluloses [29]. The bands in the region of  $1000\text{-}1125\text{cm}^{-1}$  are typical of xylan. The prominent band at  $1043\text{-}1046\text{cm}^{-1}$  is attributed to the C-C, C-O stretching vibration in hemicellulose (xylan) and is attributed to the C-OH bending vibration [28] in both holocellulose and xylan. Finally, a sharp band at  $895\text{-}899\text{cm}^{-1}$ , typical of  $\beta$ -glycosidic linkages between the sugar units in hemicelluloses, was detected in the anomeric region [30]. Thus, almost all of the absorption bands of xylan are similar to absorption bands of corn cob xylan described by Oliveira et al., 2010 [4].

### 3.2. FT-IR Spectroscopy of xylan-5-ASA ester conjugates

The FT-IR spectrum of xylan-5-ASA ester conjugates is shown in Fig.3, the most distinctive absorption bands are observed at  $1680\text{-}1685\text{cm}^{-1}$  (carbonyl stretching of ester conjugate),  $1450\text{-}1600\text{cm}^{-1}$  (C-C multiple bond stretching of aromatic ring),  $700\text{-}835\text{cm}^{-1}$  (aromatic substitution that is substituted at o- and m- position),  $1624\text{-}1630\text{cm}^{-1}$  (N-H bending of primary amino group) and  $1290\text{-}1346\text{cm}^{-1}$  (C-N stretching of primary amine) in addition to the bands originated from 5-ASA and xylan. On the basis of these spectra reaction scheme may be illustrated as in Fig.4.

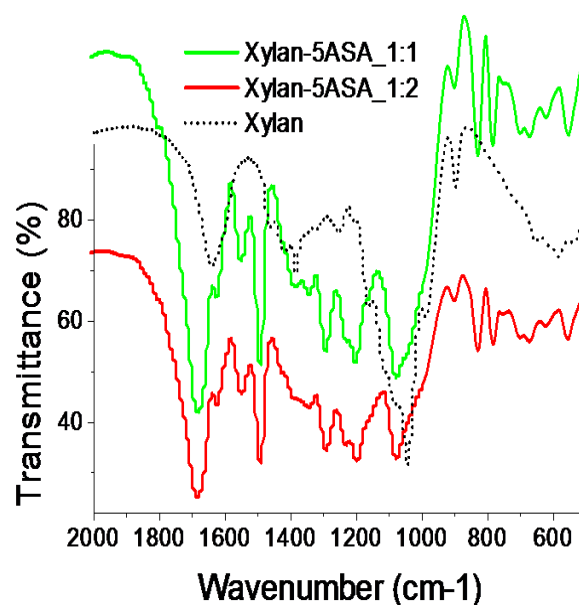
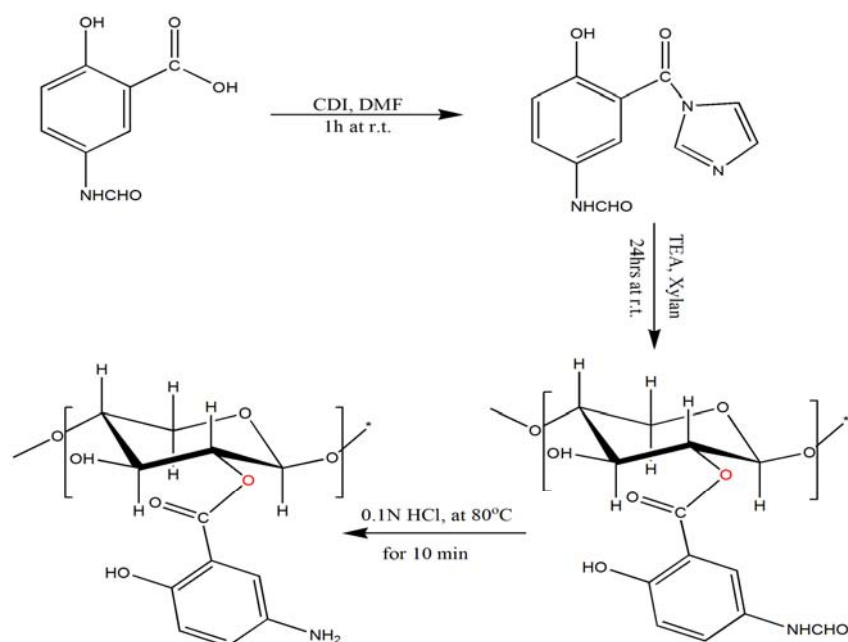


Fig.3 FT-IR spectrum of xylan-5-ASA ester conjugates



**Fig.4. Schematic representation of synthesis of xylan-5-ASA ester conjugate**

### 3.3. <sup>1</sup>H-NMR Spectroscopy of xylan and xylan-5-ASA ester conjugates

NMR experiments were conducted to elucidate the complete structure of the isolated xylan and its conjugates in TFA-d as shown in fig.5. The  $\beta$ -(1, 4)-D-xylopyranose units were characterized by the signals at  $\delta$  3.7 (H-2), 3.9 (H-5<sub>a</sub>), 4.1-4.3 (H-5<sub>c</sub>, H-4, H-3), 4.4 (H-1). Furthermore, it is noted that the two signals which are found downfield at  $\delta$  4.8 to 4.9 ppm show a weak correlation with H-3 and H-2 respectively. These signals originated from the protons of the

hydroxyl groups attached at C-3 (-C-OH) and C-2 (-C-OH) positions of the xylopyranose units in xylan. Synthesis of xylan-5-ASA ester conjugate was carried out by homogeneous reaction in DMSO/CDI/TEA system at room temperature. The structural features of ester conjugate were analyzed by employing different NMR experiments. The signals within the range of  $\delta$  3.7 to 5.0 ppm are assigned to the ring protons of xylan. The strong signals at  $\delta$  7.3 (C-11, NH<sub>2</sub>), 7.5 to 8.5 (H-10, H-9, H-12) and at  $\delta$  8.7 (C-8, -OH) confirms the successful esterification of xylan.

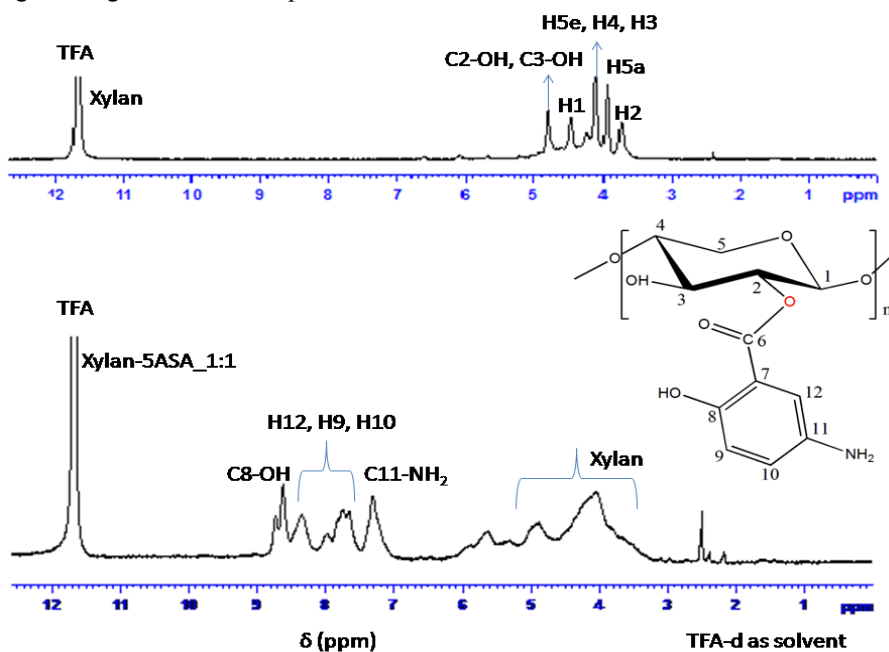


**Fig.5. <sup>1</sup>H-NMR spectra of isolated xylan and xylan-5ASA ester conjugate in TFA-d<sub>1</sub> as a solvent**

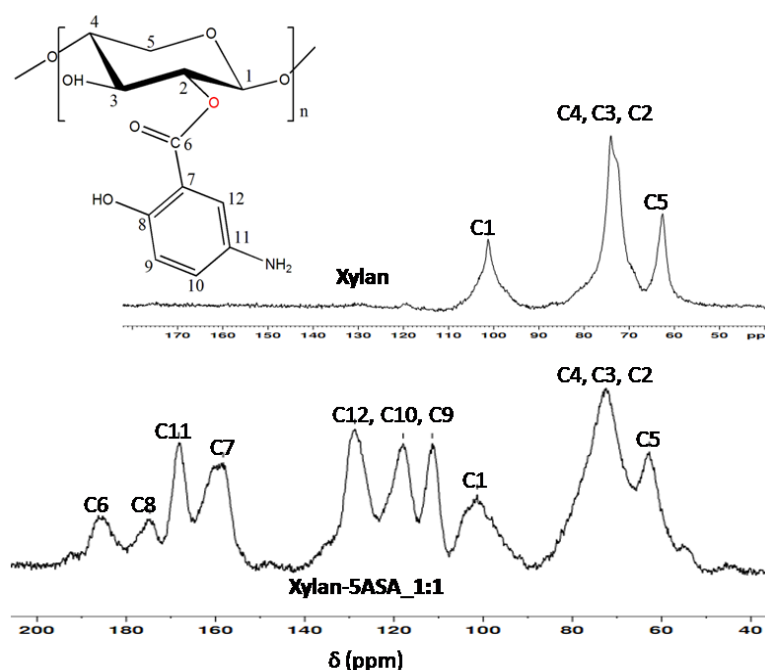


Fig.6. Solid  $^{13}\text{C}$ -NMR spectra of isolated xylan and xylan-5ASA ester conjugate

#### 3.4. Solid $^{13}\text{C}$ -NMR Spectroscopy of xylan and xylan-5-ASA ester conjugates

Solid NMR experiment was conducted to elucidate the structure of the isolated xylan and its conjugates as shown in fig.6. Major signals observed at  $\delta$  62.6 (C-5), 74.0 (C-2, C-3, C-4) and  $\delta$  101.3 ppm corresponding to C-1 of the D-xylopyranose units in xylan. No other additional signals were observed indicating that the isolated xylan does not contain any acetyl groups such as MeGlcA, neutral sugars and lignin. Acetyl groups are cleaved from its main chain during alkaline extraction. Thus, based on the above observations the isolated hemicellulose is considered as homoxylan. The solid  $^{13}\text{C}$ -NMR spectrum of xylan-5-ASA ester conjugate is presented in Fig 6. The signals at  $\delta$  62.6 (C-5), 74.0 (C-2, C-3, C-4) and  $\delta$  101.3 ppm corresponding to C-1 of the D-xylopyranose units in xylan-5-ASA ester conjugates showed the correlation of the ring carbon atoms of xylan. The signal at  $\delta$  186 ppm originates from carbonyl carbon (C-6) of ester bonds. The presence of other signals at  $\delta$  111.4, 117.9, 128.7, 158.3, 168.2 and 174.7 corresponds to C-9, C-10, C-12, C-7, C-11, and C-8 respectively may further confirm the esterification of xylan.

#### 3.5. Thermal Analysis of xylan and its ester conjugates

It is important to note that higher heating rates cannot give good results as higher heating rates result into large thermal lag and improper heat transfer which in turn would invalidate the kinetic data. Gronli et al. had also reported that the thermal decomposition should be carried out at low or moderate heating rates to keep possible heat/mass-transfer intrusions to a minimum level [31, 32]. The TG trace for 5-ASA gives a single-stage mass loss (100%) onset at about 255°C and maximum close to 296°C, corresponding to the melting point whereas, TG curve of 5-fASA gives double stage mass loss onset at about 255°C and maximum close to 269.2°C, corresponding to the melting point and second has onset at about 270°C and maximum close to 295.5°C, corresponding to thermal decomposition, as confirmed by DTG curve. The active substance 5-ASA showed a characteristic thin endothermic peak at 296.3°C representing the melting point whereas 5-fASA showed thin endothermic peak at 262.89°C indicating the melting point, analogous to Jung et al., 1998; Zou et al., 2005 [22, 23], mp: 248-251.19°C and the other at 293.6°C may be due to thermal decomposition (table 2).

Table 2: Data calculated from TG, DTG and DTA thermograms of samples at a heating rate of 10°C min<sup>-1</sup> in nitrogen atmosphere

Samples	$T_i$ (°C)	Char yield (%) at 600°C	DTG peak maxima temp (°C)	DTA maxima (°C)	Nature of DTA peak
5-ASA	255	0.2	296.3	296.3	Endo
5-fASA	255	14.7	269.2, 295.5	262.89, 293.6	Endo
XNPs	219	22.1	293	293.7	Exo
XNPs-5-ASA_1:1	157	26.9	216	219.9	Exo
XNPs-5-ASA_1:2	210	18.0	232.4	236.7	Exo

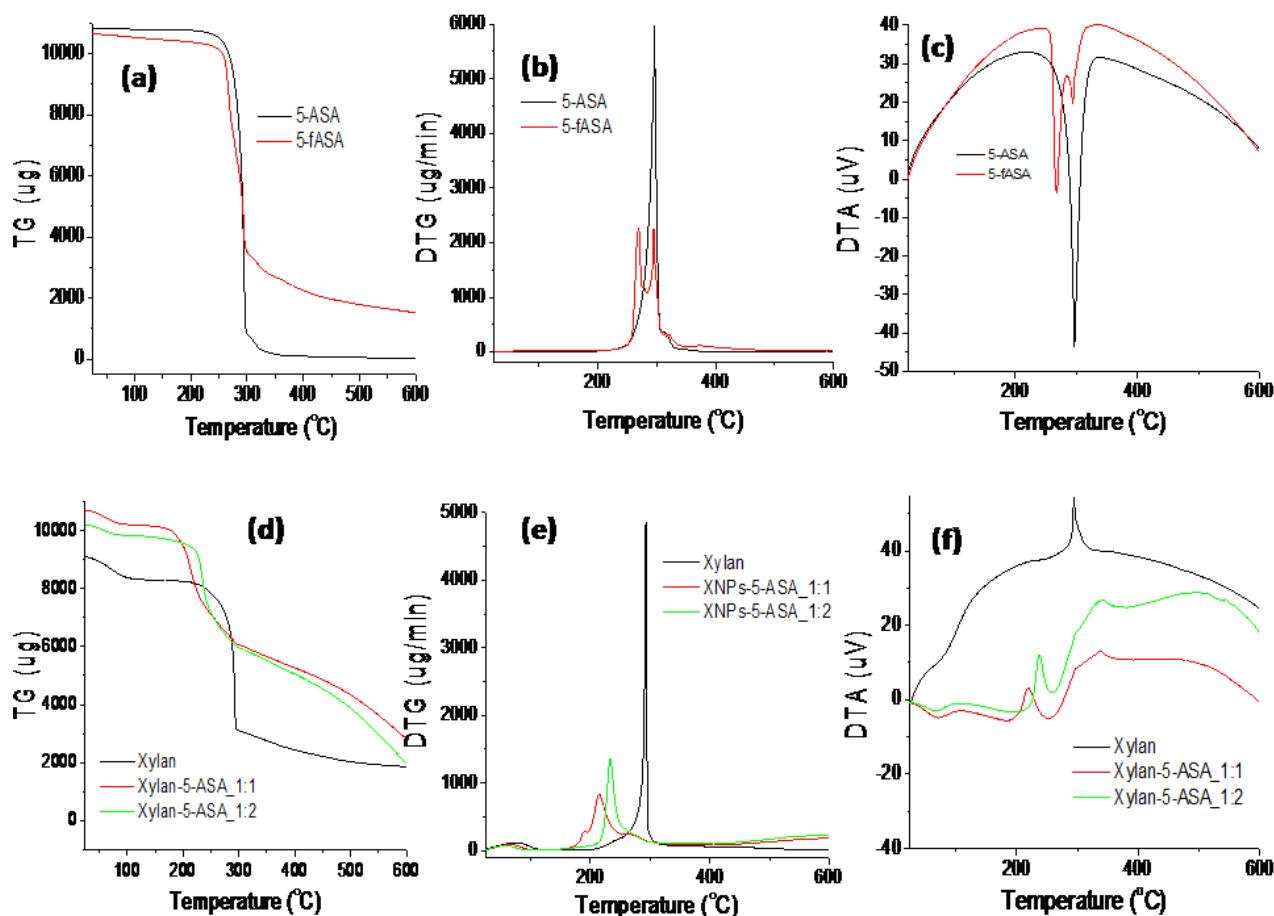


Fig.7. Shows the TG, DTG and DTA curve of 5-ASA, 5-fASA, xylan, xylan-5-ASA\_1:1 and xylan-5ASA\_1:2

Isolated xylan showed an exothermic event with peak maxima at 294.8°C (as shown in fig.7 and table2) which attributed to decomposition of polymer in the temperature range 240-320°C and there is no melting peak. The ester conjugate of xylan has also an exothermic event with small intensity broad peak at about 216°C and 232°C in case of xylan-5-ASA\_1:1 and xylan-5-ASA\_1:2 respectively. The initial decomposition temperature and DTG peak maxima temperature of ester conjugates are directly related to the degree of substitution, the conjugate with higher degree of substitution has lower char yield and higher initial decomposition and DTG peak maxima temperature in their respect as shown in table 2.

### 3.6. Powder X-ray diffraction (PXRD)

The spectra of the ester conjugates are clearly different from xylan component; it showed a less crystallization state as evidenced by single and broader peak of lower intensity. The formation of a different crystal structure may be considered as an indirect proof for inclusion of the drug in to the polymeric backbone of xylan. Attempt was made to accumulate long enough by concentrating in a region of 7–20° to obtain a signal with ester conjugates. There was no

prominent peak but broader peak was appeared, which undoubtedly confirms that 5-ASA does not re-crystallize in the xylan backbone, but it is covalently linked in the polymeric matrix at a molecular level [33].

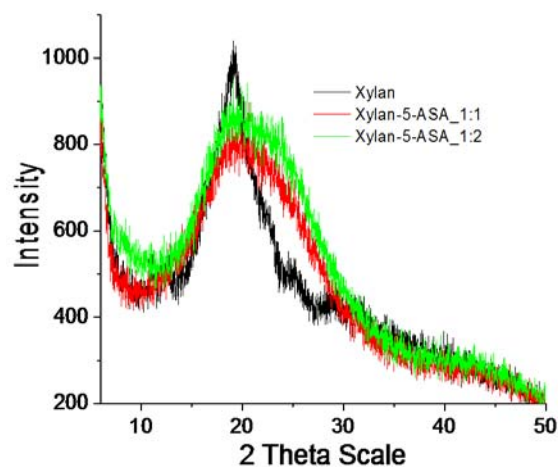
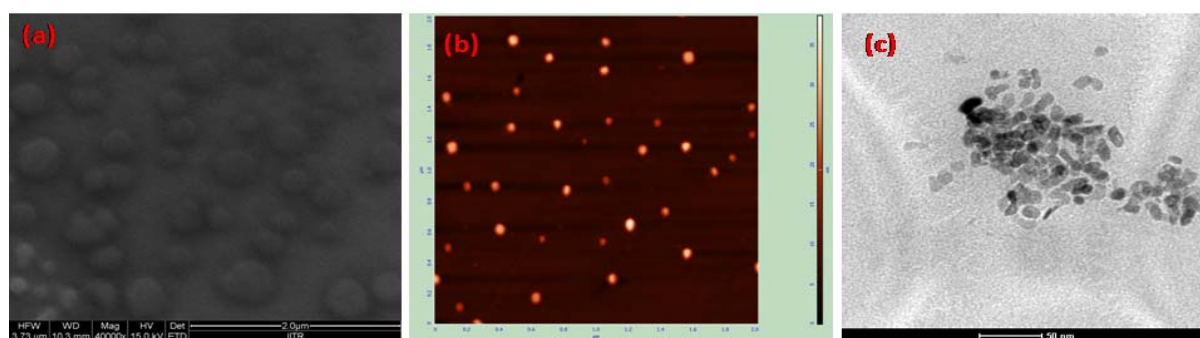


Fig.8. Powder x-ray diffractograms of xylan, xylan-5-ASA\_1:1 and xylan-5ASA\_1:2



**Fig.9.** Micrographs of ester conjugate (a) SEM (scale bar 2 $\mu$ m) (b) AFM (scale bar 2 $\mu$ m) and (c) TEM (scale bar 50nm)

### 3.6. Particle Size of Ester Prodrug of 5-ASA

Morphological evidence of the ester prodrug of 5-ASA with an average diameter of  $258\pm 87$ nm,  $54\pm 11$ nm and  $13\pm 4$ nm were measured by SEM, AFM and TEM technique respectively as shown in fig.9. An average particle size of  $258\pm 87$ nm as measured by SEM technique indicates the clustering of particles and thus the clear evidence was obtained from TEM technique. Surface area of the smaller particle becomes more and provide large surface for bacterial action in the colon part and thus it may be assumed that more and more drug will be release at specific site.

### 3.7. In vitro release studies of 5-ASA

In-vitro drug release profile of 5-ASA from ester prodrug of 5-ASA is given in fig.10 shows sustained and targeted drug release behavior. The rate of release showed dependence on the pH of the medium and polymeric microstructure. Food taken orally is stayed only for 3 to 4 hours and approximately  $\leq 2\%$  drug such as 5-ASA was released during this period at acidic pH 1.2 and rest of the drug may be gone towards upper/lower GIT in human being. Release of 5-ASA from ester prodrug becomes negligible also ( $\leq 2\%$ ) during in-vitro conditions at slightly alkaline pH 7.4, although loading of drug is satisfactory. As discussed earlier that lower part of human GIT contains  $10^{11}$ - $10^{12}$  CFU/ml (colony forming units per milliliter) microflora consisting mainly of anaerobic bacteria, e.g. Bacteroides, Bifidobacteria, Eubacteria, Clostridia, Enterococci, Enterobacteria, etc that fulfils its

energy needs by fermenting various types of substrates that have been left undigested in the small intestine. Because of the presence of these biodegradable enzymes only in the colon, the use of bacterial degradable polymers for colon specific drug delivery seems to be a more site specific approach as compared to other approaches [21]. Therefore, it may be assumed that the rest of the 98% drug will be released in the lower part of GIT. The degree of substitution also affects the release pattern of the drug as higher degree of substitution, confirms that 5-ASA may be arranged orderly in the macromolecular backbone of xylan. Jung et al have reported the release mechanism of drug molecule, may not be released from dextran-drug conjugate in the upper GIT, which may be attributed to the steric hindrance of the biopolymer matrix prevents the enzymic action there but it may be released from the oligomerized dextran-drug conjugate, which is formed by depolymerization of dextran matrix by endodextranase in the colon where the bacterial count is very high [23]. The similar mechanism may also be expected for xylan-drug (Xylan-5-ASA) conjugates for drug release from prodrug of 5-ASA. The release of drug from prodrug of 5-ASA may also be done due to the long transit through colon (30-40hs). Thus it may be assumed that the above prepared prodrug (xylan-5-ASA) might be applicable for sustained and colon-specific release for 5-ASA to avoid systemic side effect.

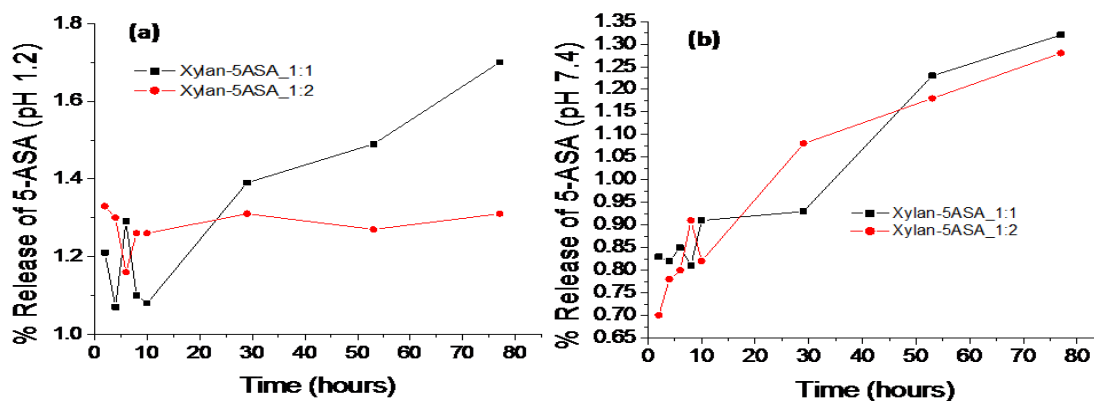


**Fig.10.** Shows the release profile of drug such as 5-ASA from respective ester prodrug

#### 4. CONCLUSIONS

Xylan, a green biopolymer may be useful in the pharmaceutical field, especially for the synthesis of colon-specific drug carriers, such as micro- and nanoparticles. Thus the synthesized ester prodrug (xylan-5-ASA) might be applicable for sustained and site specific to avoid systemic side effect. Preparation of xylan prodrug could be an important issue concerning to the environment because a green biopolymer from a renewable source was in fact a great competitor for the pharmaceutical industrial research and development sectors.

#### ACKNOWLEDGEMENTS

One of the authors, Mr. Samit Kumar is highly thankful to the Ministry of Human Resource Development (MHRD), New Delhi, India for the financial research grant for pursuing the Ph.D. work.

#### REFERENCES

- [1] Kumar, S., Negi, Y. S., Upadhyaya, J. S., *Adv. Mater. Lett.* 2010a 1, 246-253.
- [2] Garcia, R. B., Nagashima, J. T., Praxedes, A. K. C., Raffin, F. N., Moura, T. F. A. L., Egito, E. S. T. do., *Polym. Bull.*, 2001, 46, 371-379.
- [3] Kumar, S., Upadhyaya, J. S., Negi, Y. S., *BioResources*. 2010b 5, 1292-1300.
- [4] Oliveira, E. E., Silva, A. E., Júnior, T. N., Gomes, M. C. S., Aguiar, L. M., Marcelino, H. R., Araújo, I. B., Bayer, M. P., Ricardo, N. M. P. S., Oliveira, A. G., Egito, E. S. T., *Bioresour. Technol.*, 2010, 101, 5402-5406.
- [5] Kumar, V., de la Luz Reus-Medina, M., Yang, D., *Int. J. Pharm.*, 2002, 235, 129-140.
- [6] Wells, J.I., In: Horwood, E. (Ed.), *Pharmaceutical Preformulation: The Physicochemical Properties of Drug Substances*. Halsted Press, Chichester, New York, 1988.
- [7] Carr, L.L., *Classifying flow properties of solids*, Chemical Engineering, 1995.
- [8] Daggupati, V. N., Naterer, G. F., Gabriel, K. S., Gravelins, R. J., Wang, Z. L., *Int. J. Hydrogen Energy*, 2011, 36, 11353-11359.
- [9] Silva, A. E., Marcelino, H. R., Gomes, M. C. S., Oliveira, E. E., Nagashima Jr, T., Egito, E. S. T., in: Verbeek, C. J. R., E-Publishing InTech Janeza Trdine Rijeka., Croatia, 2012 pp.61-84
- [10] Ünlu, C. H., Günister, E., Atici, O., *Carbohydr. Polym.*, 2009, 76, 585-592
- [11] Pauly, M., Keegstra, K., *Curr Opin Plant Biol.* 2010, 13, 1-8.
- [12] Ebringerova, A., Hromadkova, Z., Hribalova, V., *Int. J. Biol. Macromol.*, 1995, 17, 327-331.
- [13] Ebringerova, A., Hromadkova, Z., Kacurakova, M., Antal, M., *Carbohydr. Polym.* 1994, 24, 301-308.
- [14] Hromadkova, Z., Kovacicova, J., Ebringerova, A., *Ind Crop Prod.* 1999, 9, 101-109.
- [15] Silva, A. K. A., Silva, E. L., Oliveira, E. E., Nagashima, J. T., Soares, L. A. L., Medeiros, A.C., Araujo, J. H., Araujo, I. B., Carriço, A. S., Egito, E. S. T., *Int J Pharm*, 2007, 334, 42- 47.
- [16] Daus, S., Heinze, T., *Macromol. Biosci.* 2010, 10, 211-220.
- [17] Moore, W.E.C., Holdeman, L.V., *Cancer Res.* 1975, 35, 3418-3420.
- [18] Rubinstein, A., *Biopharm Drug Dispos.* 1990, 11, 465-475.
- [19] Cumming, J.H., Englyst, H.N., *Am. J. Clin. Nutr.* 1987, 45, 1243-1255.
- [20] Scheline, R.R., *Pharmacol. Rev.*, 1973, 25, 451-523.
- [21] Sinha, V.R., Kumria, R., *Int J Pharm* 2001, 224, 19-38
- [22] Zou, M., Okamoto, H., Cheng, G., Hao, X., Sun, J., Cui, F., Danjo, K., *Eur J Pharm Biopharm.*, 2005, 59, 155-160.
- [23] Jung, Y. J., Lee, J. S., Kim, H. H., Kim, Y. T., Kim, Y. M., *Arch Pharm Res.* 1998, 21, 179-186.
- [24] Rubinstein, A., *Biopharm. Drug Dispos.*, 1990, 11, 465-475.
- [25] Yadav, R., Mahatma, O. P., *J. Pharm. Sci. & Res.*, 2011, 3, 966-972.
- [26] Meryandini, A., Sunarti, T. C., Mutia, F., Gusmawati, N. F., Lestari, Y., *J. Appl. Indus. Biotechnol. Tropical Region*, 2009, 2, 1-6.
- [27] Sun, X. F., Zhao, F. X. H., Sun, R. C., Fowler, P., Baird, M. S., *Bioresour. Technol.*, 2005, 96, 1342-1349.
- [28] Colom, X., Carrillo, F., Nogue's, F., Garriga, P., *Polym Degrad Stabil.* 2003, 80, 543-549.
- [29] Sun, R. C., Fang, J. M., Goodwin, A., Lawther, J. M., Bolton, A. J., *Carbohydr. Polym.* 1998, 37, 351-359.
- [30] Sun, R. C., Tomkinson, J., *Int J Polym Anal Ch*, 1999, 5, 181-193.
- [31] Grønli, M. G., Varhegyi, G., Di Blasi, C., *Ind Eng Chem Res.* 2002, 41, 4201-4208.
- [32] Arora, S., Lal, S., Kumar, S., Kumar, M., Kumar, M., *Arch. Appl. Sci. Res.*, 2011, 3, 188- 201
- [33] Mladenovska, K., Cruaud, O., Richomme, P., Belamie, E., Raicki, R. S., Venier-Julienne M. C., Popovski, E., Benoit, J. P., Goracinova, K., *Int J Pharm*, 2007,345, 59-69.